ELSEVIER

Journal of Hazardous Materials 57 (1998) 193–207

JOURNAL OF HAZARDOUS MATERIALS

Gas-phase adsorption isotherms and mass transfer characteristics of 1,1-dichloro-1-fluoroethane (HCFC-141b) by various adsorbents

Sheng H. Lin *, Yu W. Chen

Department of Chemical Engineering, Yuan Ze Institute of Technology, Neili, Taoyuan 320, Taiwan, People's Republic of China

Received 15 April 1997; accepted 30 June 1997

Abstract

Experiments have been conducted to investigate gas-phase adsorption characteristics of 1,1-dichloro-1-fluoroethane (HCFC-141b) by activated carbon fiber (ACF), extruded activated carbon (EAC), granular activated carbon (GAC), activated alumina and molecular sieve. HCFC-141b is currently regarded as an excellent replacement for CFC-11, a foaming agent widely used in the rigid polyurethane foam industries. Performances of HCFC-141b adsorption were characterized by the equilibrium adsorption capacity, time to reach equilibrium and desorption efficiency of adsorbent. A simple thermal treatment process with proper operating temperature and treatment duration was found to be effective for pretreatment of fresh adsorbents and regeneration of exhausted ones. The empirical Freundlich adsorption isotherm was observed to adequately represent the equilibrium adsorption data. A mass transfer model based on the pseudo steady state squared driving force was adopted to describe the mass transfer process of HCFC-141b adsorption. © 1998 Elsevier Science B.V.

Keywords: Gas-phase adsorption; HCFC-141b; Various adsorbents; Adsorption isotherms; Mass transfer model

1. Introduction

Molina and Rowland [1] were the two scientists who first found that depletion of atmospheric ozone was related to extensive uses of chlorofluorocarbons (CFCs) on earth. The ozone destruction by various CFCs had led to appearance of holes in the

* Corresponding author.

PII S0304-3894(97)00081-2

ozone layer over the Arctic and Antarctic and thinning of ozone layer surrounding the earth also [2]. Such a CFC-mediated depletion of ozone layer results in a significantly increased intensity of UV light on earth which has been shown to cause severe and adverse environmental impacts on human beings and other living organisms [2,3]. This has prompted the United Nations Environmental Program (UNEP) to formulate the Montreal Protocol which calls for gradual reduction and eventually phase-out of worldwide production/use of CFCs and identification of ozone-compatible CFC replacement compounds [2–5].

Among the various measures to minimize the adverse environmental impacts of CFC, one important issue receiving increasing amount of attention in recent years is safe disposal of CFCs currently in use. Because CFCs are highly stable chlorine- and fluorine-containing organic compounds, safe disposal of all CFCs is not easy. Incineration or chemical destruction have been popular methods and extensive investigations have been conducted by many researchers to examine various facets of incineration and chemical destruction [6–23]. A major disadvantage of incineration or chemical destruction of CFCs is that chlorinated compounds generated in the process could cause significant air pollution problem which need to be carefully addressed. A possible alternative to incineration or chemical destruction of CFCs is their removal by adsorption, a method which has not received much attention in the past. Adsorption of CFCs or related compounds does not produce any adverse consequence and allows recovery of adsorbed compounds for reuse.

The purpose of this paper was to investigate gas-phase adsorption of 1,1-dichloro-1-fluoroethane (HCFC-141b) by various adsorbents, including activated carbon fiber (ACF), extruded activated carbon (EAC), granular activated carbon (GAC), activated alumina and molecular sieve. Due to its relatively low ozone depletion potential (ODP) and global warming potential (GWP), HCFC-141b is currently regarded as an excellent replacement for foaming agent CFC-11 in the manufacturing of various polyurethane foams (soft or rigid). It is also used as a substitute for CFC-113 and 1,1,1-trichloroethane (CCl_3-CH_3) which were very popular cleaning agents employed in the electronic and precision machine industries. In the present study, experiments were conducted to evaluate the gas-phase adsorption and desorption performance characteristics of HCFC-141b by those adsorbents. Adsorption isotherms and mass-transfer modeling were also considered. The results of the present investigation would help elucidate the possibility of HCFC recovery by an adsorption process.

2. Experimental

The granular activated carbon (GAC) employed here was the regular type, as obtained from Cheng Tai Chemical Co., Taichung, Taiwan. This GAC was industrial grade and made from coconut shells. It was highly irregular in both shape and size. According to the manufacturer, the GAC had an average diameter of 5 mm and a density of 0.45 g/cm^3. Its BET surface area was measured by a Micromerites porosimeter (Model ASAP 200, Micromerites Instrument Corp., Norcros, GA) to be 905 m^2/g with an average pore diameter of 26 A. This grade of GAC is widely used in the chemical

Table 1
Properties of activated carbon fiber (ACF-1300)

Thickness, cm	0.061
Weight, g/cm^2	80
BET surface area, m^2/g	1152
Pore volume, ml/g	0.6–0.7
Pore diameter, A	8–10

and food process industries for various adsorption, decolorization and pollution abatement purposes. The second type of activated carbon was the extruded pellet (Sorbonorit B4), as obtained from Norit Ltd. of the Netherlands. It has a density of 0.41g/cm^3, a measured BET surface area of 1147 m^2/g and an average dimensions of 3.6 mm (D) × 6.2 mm (L).

The activated carbon fiber (ACF) was obtained from Neolite Technical Co., Taipei, Taiwan. It was made of polyacrylonitrile (PAN). The PAN-based ACF was regarded by many previous investigators [24–27] to be an excellent one among the various ACFs commercially available. The properties of activated carbon fiber (type ACF-1300) as provide by the manufacturer are listed in Table 1. The activated alumina (Type A4-8) was obtained from Procatalyse Co., Rueil Malmaison, France. It has a measured BET surface area about 270 m^2/g and a bulk density of 770 kg/m^3. Its aluminum oxide (Al_2O_3) content is greater than 93.5%. The molecular sieve (Zeolum 10A) was obtained from Rhone-Poulenc Chimie, France with a BET surface area of 237 m^2/g.

The HCFC-141b employed was obtained from Daikin Chemical Industries, Ltd. (Osaka, Japan). Table 2 compares the physical properties of HCFC-141b and CFC-11. It is apparent that there is a strong similarity in physical properties between the two organic compounds which may partially account for the good replacement capability of HCFC-141b for CFC-11.

To determine the maximum adsorption capacity of each adsorbent, an excessive amount of HCFC-141b liquid was placed in a 200-ml flask. After being well sealed, the flask was placed in a constant temperature bath for at least an hour to equilibrate the temperature and to completely saturate the headspace in the flask. The seal was open and a small amount of pretreated adsorbent was placed and suspended in the flask. The flask was resealed to start the adsorption and left in the constant temperature bath for at

Table 2
Physical properties of HCFC-141b and CFC-11

Item	HCFC-141b	CFC-11
Chemical formula	$CHCl_2$-CH_2F	CCl_3F
Molecular weight	116.95	137.37
Boiling point, °C	32.1	23.8
Freezing point, °C	−103.5	−111.0
Density at 25°C, g/m	1.235	1.476
Solubility in water at 25°C, mg/l	420	110.0
Viscosity at 25°C, cP	0.43	0.41
Evaporation latent heat, cal/g	52.3	43.1
Ozone Depletion Potential (ODP)	0.11	1

least six hours. The flask was open after that and the saturated adsorbent was placed in a small plastic bag to minimize the evaporation loss of adsorbed HCFC-141b. The amount of equilibrium adsorption was determined. Due to all precautional measures taken to minimize possible errors involved, the maximum amount of HCFC-141b adsorption was consistent (maximum loading within 3% for five samples), and the average was accepted as the maximum adsorption capacity.

For the isotherm studies, a given amount of pretreated adsorbent was suspended in the flask which was then sealed and placed in the constant temperature bath. A small amount of HCFC-141b was injected into the flask. The HCFC-141b was completely vaporized almost instantaneously after injection. Gaseous samples were taken to measure the HCFC-141b concentration using a HP 5890 gas chromatograph with capillary column and FID detector (Hewlett Packard Instruments, Inc., CO). The flask was left in the constant temperature bath for at least six hours and the gaseous sample was taken again to measure the residual HCFC-141b concentration. In each test run, three flasks were employed to insure the accuracy of measured data. The test runs were repeated with various initial amounts of HCFC-141b injection and were run at several temperatures.

After adsorption experiments were completed, the desorption tests were conducted. In the desorption tests, the exhausted adsorbents were put in an electric oven which was maintained at constant temperature (± 1°C). The weight loss of the adsorbent samples was determined periodically. Desorption was considered complete after there was no more weight change in the adsorbent samples being treated. Various desorption temperatures were explored and an optimal temperature was chosen on the basis of achieving efficient desorption in a short time. The desorption test runs of exhausted adsorbent usually lasted more than four hours. At the end of a desorption run, the treated adsorbent was placed in a desiccator for cooling for over two hours until it reached room temperature (approximately 25°C). The weight of adsorbent was quickly weighed before the next round of adsorption experiments began. Each cycle of adsorption/desorption test run was repeated at least twice to ensure the reproducibility and accuracy of the test data collected.

3. Discussion and results

At the beginning of the adsorption experiments, all activated carbon adsorbents (GAC, EAC and ACF) must be treated to remove all impurities which might have been adsorbed on the pore surfaces. The same desorption process was also performed to regenerate the exhausted adsorbents for reuse. For the present work, a simple thermal desorption process was adopted with which exhausted adsorbents were heat treated in an vacuum electric oven. Determination of an optimal desorption temperature is thus important. The top graph of Fig. 1 shows the ACF-1300 and GAC desorption efficiencies as a function of temperature. The desorption efficiency was defined as follows:

$$\text{Desorption Efficiency } (\%) = \frac{D - D_f}{D_0 - D_f} \times 100 \tag{1}$$

where D_0 is the initial weight of exhausted adsorbent before desorption, D_f the final

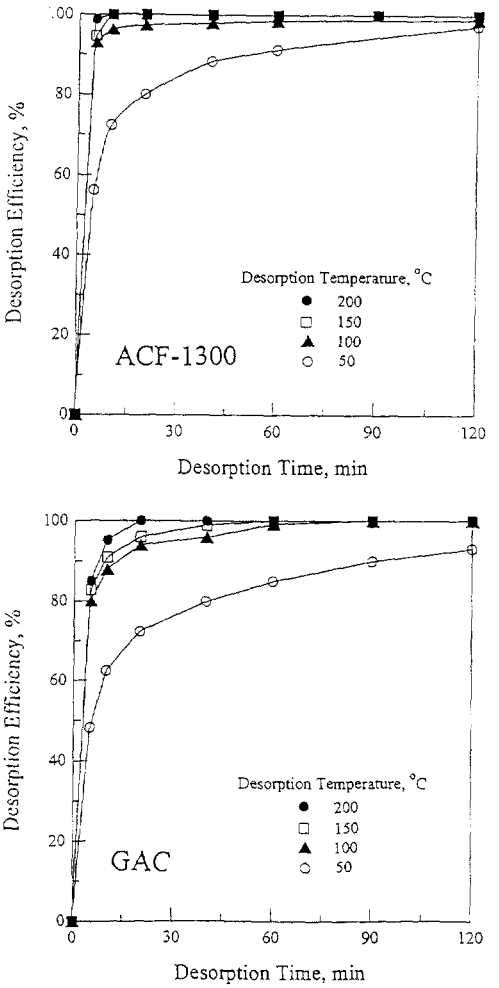

Fig. 1. Thermal desorption efficiency of ACF-1300 and GAC as a function of temperature.

weight and D the weight at any sampling time. Hence the percent desorption efficiency in this graph represented the extent an exhausted adsorbent had been restored to the original weight. It is apparent that below 100°C, complete desorption is very difficult to achieve due presumably to insufficient amount of energy supplied to sever the bonds between the adsorbed organic compound and the adsorption sites. But as the electric oven temperature was raised to 150°C and above, desorption was completed in less than one half hour. Such desorption characteristics were observed for other activated carbon and non-carbon adsorbents also. At 150°C, the desorption curves for all adsorbents employed are shown in Fig. 2. As shown, desorption was complete in less than two hours. Hence the operating conditions (150°C and two hours) were adopted for desorption of exhausted adsorbents as well as pretreatment of fresh ones.

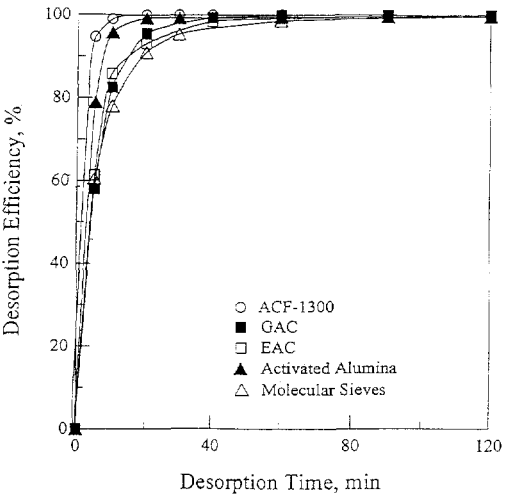

Fig. 2. Thermal desorption efficiency of various adsorbents as a function of time at 150°C.

Fig. 3 displays the amounts of HCFC-141b adsorbed by various adsorbents as a function of time. On the basis per unit adsorbent weight, ACF-1300 outperforms by a significant margin EAC which in turn outweighs GAC, activated alumina and molecular sieve. It is also noted here that the adsorption curves for activated carbons (ACF, EAC and GAC) taper off much earlier than those for the two non-carbon adsorbents, implying more rapid adsorption speed for these adsorbents. In general, all adsorbents were

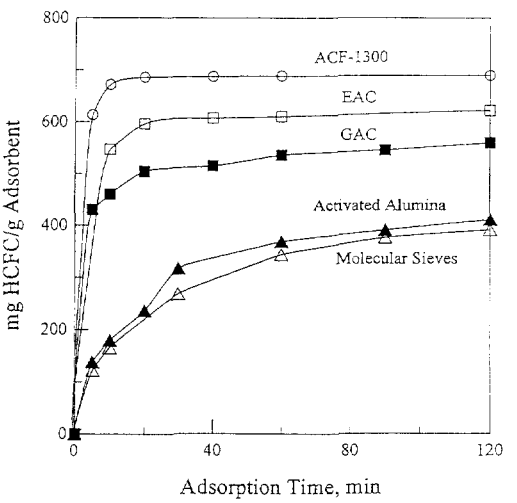

Fig. 3. Adsorption capacities per unit weight of adsorbent of various adsorbents at 25°C.

completely exhausted in less than six hours because no more weight change of adsorbent was observed in the tests. The same adsorption data given in Fig. 3 were recalculated in terms of BET surface area of each adsorbent. On this basis, the adsorption data were displayed in Fig. 4. It is of interest to note that the adsorption capacities of adsorbents shown in Fig. 3 were reversed. The adsorption per unit BET surface area of molecular sieve or activated alumina, which were the two worst on the per unit weight basis, were highest, exceeding those of activated carbon adsorbents. The HCFC-141b adsorption capacities demonstrated in this figure appear in two distinct groups with molecular sieve and activated alumina in one and all activated carbons in the other. The reason is not known. It could be due to the fact that the two non-carbon adsorbents in general have bigger pores which permit easier excess to the adsorption sites for HCFC-141b. Regardless of the higher HCFC-141b adsorption capacity of non-carbon adsorbents on the per unit BET surface area basis, it is still difficult to judge which adsorbent type is more economic for practical applications because the cost factor has not been considered here.

Temperature has been known to negatively influence adsorption of organic compounds by GAC [28]. This is due mainly to the fact that adsorption of organic compounds is an exothermic process and a higher temperature tends to weaken the bonding between the organic compounds and the active adsorption sites. Such a temperature effect on the HCFC-141b adsorption capacities of ACF-1300 and GAC is demonstrated in Fig. 5 in the temperature range between 10°C and 25°C. As seen in this figure, the temperature effect on HCFC-141b adsorption by ACF-1300 and GAC are not very large, less than 4% and 3.2%, respectively, at 10°C and 25°C. The equilibrium adsorption capacities of the adsorbents can be correlated very well to temperature by:

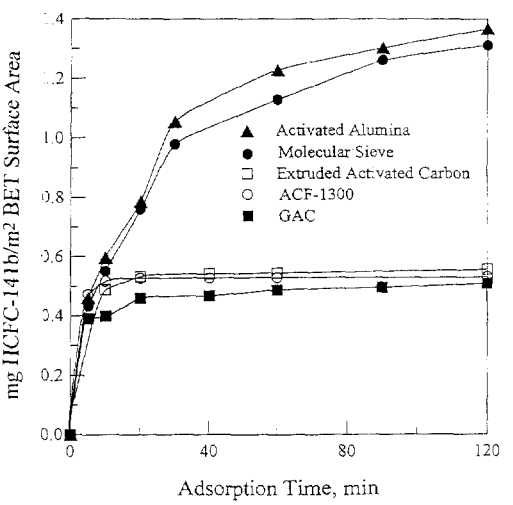

Fig. 4. Adsorption capacities per unit BET surface area of adsorbent of various adsorbents at 25°C.

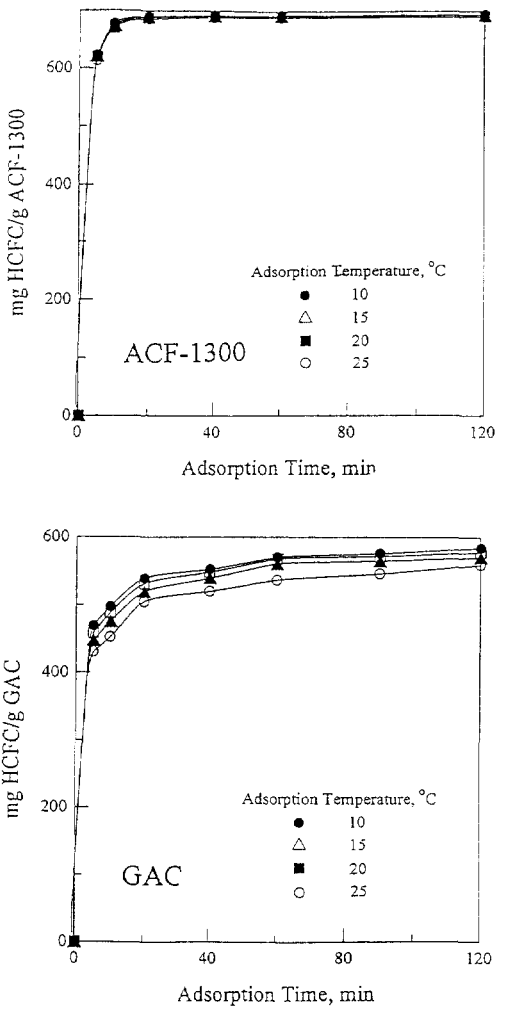

Fig. 5. Temperature effect on the HCFC-141b adsorption capacities of ACF-1300 and GAC.

For ACF-1300,

$$Q_e = 86.9 \exp\left(\frac{587}{T}\right). \tag{2}$$

For GAC,

$$Q_e = 82.5 \exp\left(\frac{218}{T}\right) \tag{3}$$

where Q_e is the equilibrium adsorption capacity (mg HCFC/g of adsorbent) and T the temperature (K). In fact, similar temperature effects were also observed for equilibrium

HCFC-141b adsorption by activated alumina and molecular sieve. Between 10°C and 25°C, the temperature effect was observed to be less than 5%.

The two general adsorption isotherms can be represented by the well known monolayer Langmuir and empirical Freundlich models as [29,30]

$$\text{Langmuir:} \quad Q_e = \frac{ABC_e}{1 + BC_e} \tag{4}$$

$$\text{Freundlich:} \quad Q_e = KC_e^{1/n} \tag{5}$$

where C_e is the HCFC-141b concentration at equilibrium (mg/l), and A, B, K and n are constant parameters to be determined. The equilibrium HCFC-141b concentration (C_e) in the gas phase was measured by a HP 5890 GC after the adsorption equilibrium was reached. With known initial HCFC-141b concentration (C_0) and the amount of

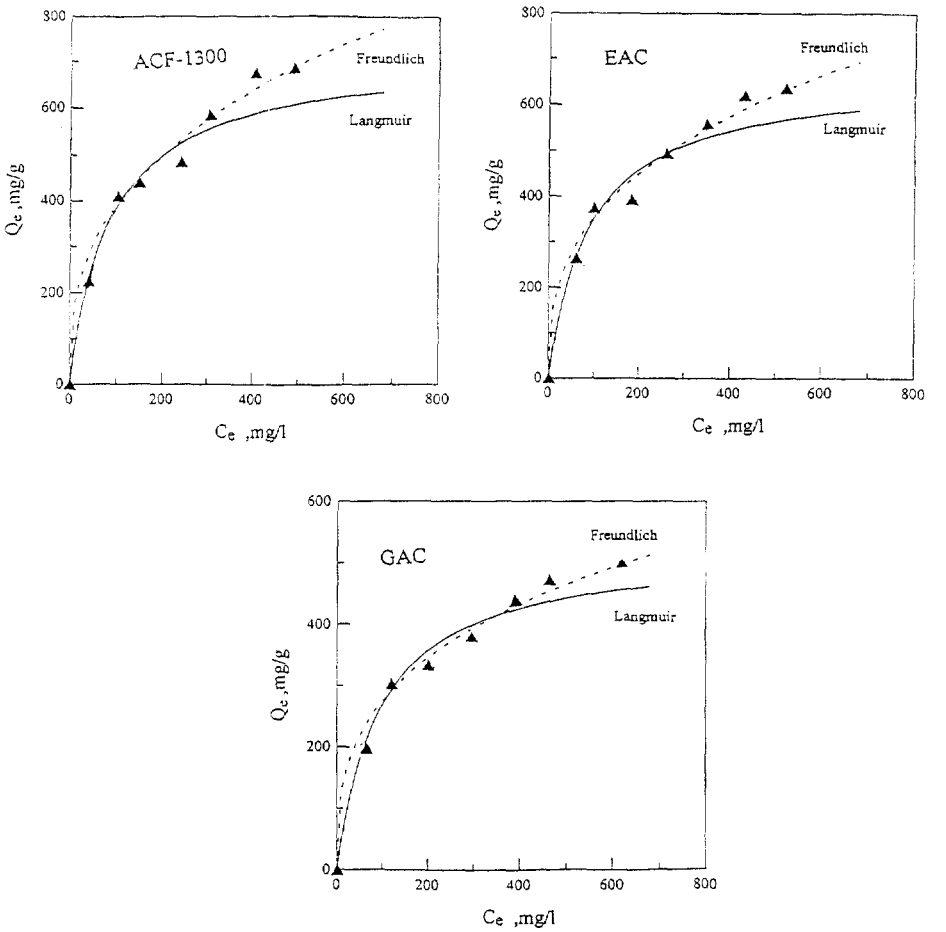

Fig. 6. Comparison of the model fit of adsorption isotherms for activated carbon adsorbents at 25°C.

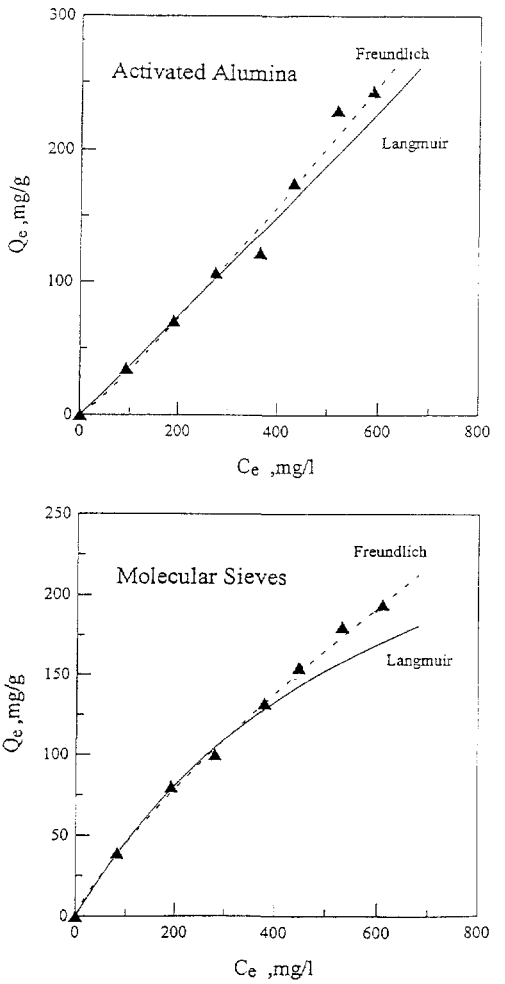

Fig. 7. Comparison of the model fit of adsorption isotherms for activated alumina and molecular sieve at 25°C.

adsorbent, the equilibrium adsorption capacity (Q_e) was easily determined. Using the equilibrium adsorption data (Q_e and C_e), the isotherm parameters in Eqs. (4) and (5) can be obtained by plotting C_e/Q_e versus $1/C_e$ and $\ln(Q_e)$ versus $\ln(C_e)$. Figs. 6 and 7 compare the observed and the predicted equilibrium HCFC-141b adsorption capacities by Eqs. (4) and (5) for activated carbon and non-carbon adsorbents, respectively. It is apparent that the Freundlich isotherm fits the observed data more closely than the Langmuir isotherm. The parameters obtained for the isotherms of various adsorbents are listed in Table 3.

Adsorption of HCFC-141b by an adsorbent is governed by mass transfer between the gas and solid phases. Several potential mass transfer resistances could be involved in this transfer process between the two phases. Models of varying complexity has been

Table 3
Isotherm parameters for various adsorbents

	Freundlich	
	k	n
GAC	61.04	3.06
Extruded activated carbon	68.77	2.82
ACF-1300	74.48	2.79
Activated alumina	0.19	0.89
Molecular sieve	1.07	1.23

proposed for describing the mass transfer process [29,30]. The pseudo steady state squared driving force model employed here can be represented by [30]

$$\frac{dC_s}{dt} = KC(C_s^* - C_s) \tag{6}$$

where C_s is the HCFC-141b concentration in the solid phase (adsorbent) at time t, C_s^* the equilibrium HCFC-141b concentration, C the HCFC-141b concentration in the gas phase and K the empirical rate coefficient. It should be noted that in formulating the above equation, the HCFC-141b concentration in the solid phase is assumed to be uniform and C_s^* was computed from the equilibrium HCFC-141b adsorption capacity (Q_e). A simple HCFC-141b balance would yield

$$C_s V_s = (C_0 - C)V_g \tag{7}$$

where V_s and V_g are the volumes of solid and gas phases, respectively, C_0 the initial

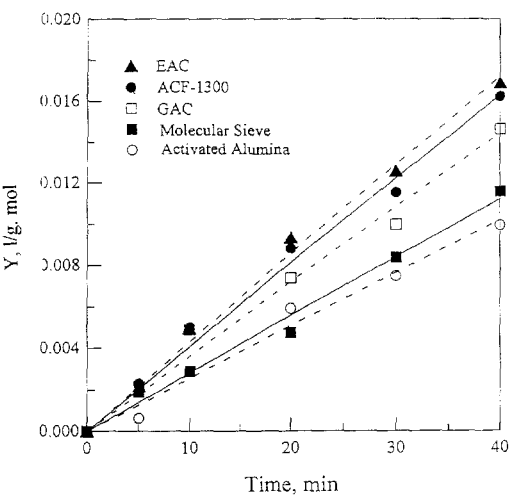

Fig. 8. Comparison of the theoretical predictions by the adopted mass transfer model and the experimental data for various adsorbents at 25°C.

HCFC-141b concentration in the gas phase and C the measured HCFC-141b concentration in the gas phase at time t. Using Eq. (7), integration of Eq. (6) yields

$$\frac{1}{C_0 - mC_s^*} \ln\left[\frac{C_s^*(C_0 - mC_s)}{C_0(C_s^* - C_s)}\right] = Y = Kt \tag{8}$$

where m is the volume ratio (V_g/V_s). Using Eq. (8), a plot of the left hand quantity, as represented by Y, against t would yield a straight line with a slope equivalent to K. Fig. 8 displays such a plot of Y versus t for various adsorbents. As shown, the experimental data do follow reasonably well the linear Y versus t relationship. Hence adoption of the

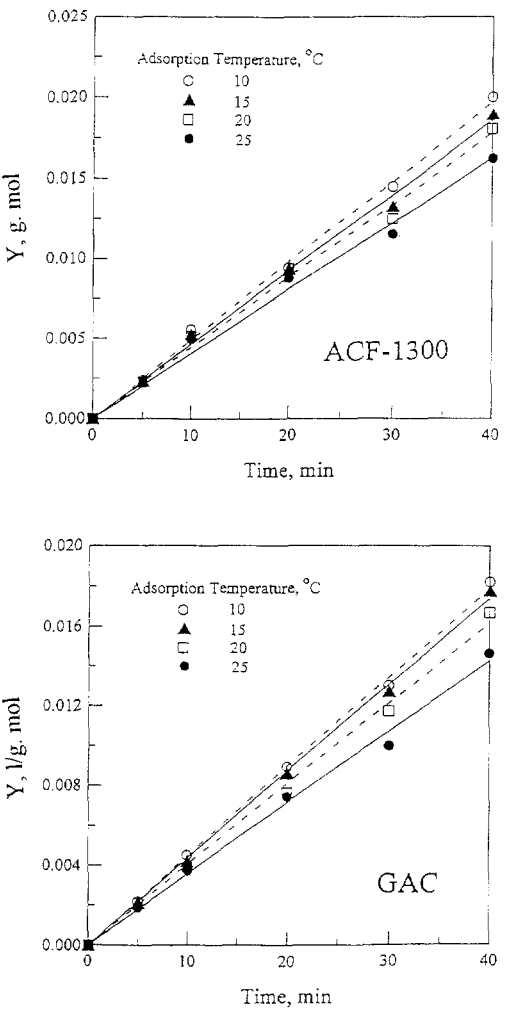

Fig. 9. Comparison of the theoretical predictions by the adopted mass transfer model and the experimental data for ACF-1300 and GAC at various temperatures.

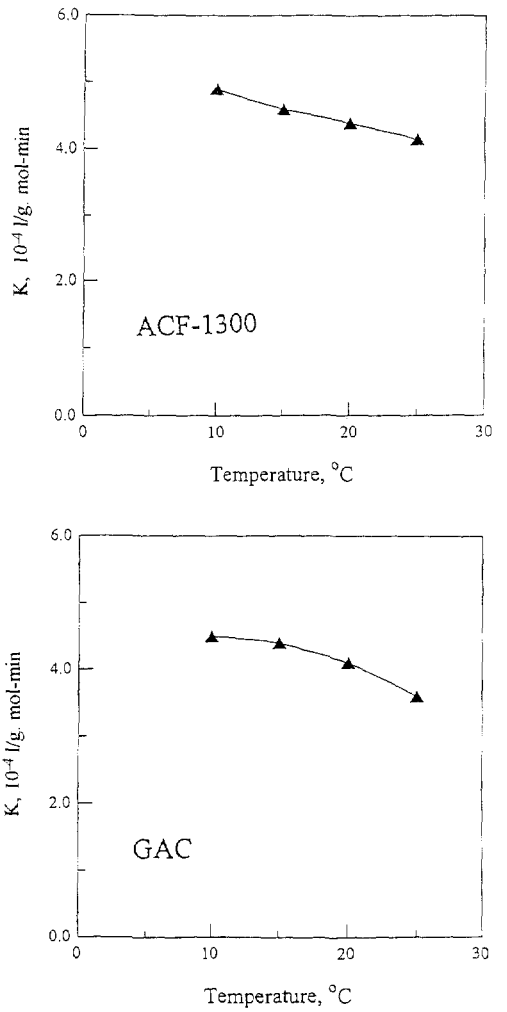

Fig. 10. Empirical mass transfer rate coefficient of HCFC-141b adsorption by ACF-1300 and GAC as a function of temperature.

pseudo steady state squared driving force mass-transfer model, as represented by Eq. (5), is justified. Plots of Y versus t for various temperatures are shown in the top and bottom graphs in Fig. 9 for ACF-1300 and GAC, respectively. The empirical mass transfer rate coefficients obtained from Fig. 9 as a function of temperature is displayed in Fig. 10. An accelerated decrease in K with increasing temperature is apparent here.

4. Conclusions

Experimental investigations were conducted to examine gas-phase adsorption of HCFC-141b by various adsorbents including activated carbon fiber (ACF), extruded

activated carbon (EAC), granular activated carbon (GAC), activated alumina and molecular sieve. Desorption tests of exhausted adsorbents by a simple thermal process have indicated that operating conditions of 150°C and two-hour thermal treatment are sufficient to achieve over 99% desorption efficiency. The adsorption test results revealed that six hours are more than sufficient for HCFC-141b adsorption to reach final equilibrium. On the per unit weight basis, the HCFC-141b adsorption capacity was found to follow the order ACF > EAC > GAC > activated alumina > molecular sieve. On the basis of per unit BET surface area, however, activated alumina and molecular sieve outperforms all activated carbon adsorbents (ACF, EAC and GAC) by a significant margin. On the latter basis, two distinct groups of HCFC-141b adsorption efficiency were observed with activated alumina and molecular sieve in one group and all activated carbon adsorbents in the other. The temperature effect on the equilibrium amount of HCFC-141b adsorbed was seen to be relatively small within the temperature range between 10°C to 25°C. An exponential relationship between the equilibrium adsorption capacity and the reciprocal of temperature was observed.

The tests results also showed that HCFC-141b adsorption by all adsorbents can be described only fairly well by the Freundlich isotherm. In the mathematical modeling aspect, a simple mass transfer model based on a pseudo steady state squared driving force principle was employed and found to describe the present mass transfer process of HCFC-141b adsorption by ACF-1300 and GAC. The empirical mass transfer rate coefficients determined from model fit to the experimental data were found to be temperature dependent.

References

[1] M.J. Molina, F.S. Rowland, Nature 249 (1974) 810.
[2] K. Wolf, J. Environ. Sci. 10 (1989) 41.
[3] J.B. Kerr, Environ. Sci. Technol. 28 (1994) 514A.
[4] M.O. McLinden, D.A. Didion, ASHRAE J. 29 (1987) 72.
[5] R.C. Barnett, ASHRAE J. 34 (1992) 134.
[6] A.J. Colussi, V.T. Amorebieta, J. Chem. Soc. Faraday Trans. 83 (1987) 3055.
[7] D.M. Blake, Int. J. Refrig. 11 (1988) 239.
[8] A. Oku, K. Kimura, M. Sato, Ind. Eng. Chem. Res. 28 (1989) 1055.
[9] T. Aida, R. Higuchi, H. Niyama, Chem. Lett. (1990) 2247.
[10] S. Imamura, T. Shiomi, S. Ishida, K. Utani, Ind. Eng. Chem. Res. 29 (1990) 1758.
[11] S. Imamura, K. Imakubo, S. Furuyoshi, H. Jindai, Ind. Eng. Chem. Res. 30 (1991) 2355.
[12] S. Imamura, H. Shimizu, T. Haga, S. Tsuji, K. Utani, M. Watanabe, Ind. Eng. Chem. Res. 32 (1993) 3146.
[13] S. Miyatani, K. Shinoda, T. Nakamura, M. Ohta, K. Yasuda, Chem. Lett. (1992) 1901.
[14] K. Ogura, W. Kobayashi, C. Migita, K. Kakum, Environ. Technol. 13 (1993) 81.
[15] S. Karmakar, H.L. Greene, J. Cat. 138 (1992) 364.
[16] G.M. Bickle, T. Suzuki, Y. Mitarai, Appl. Catalysis B: Environ. 4 (1994) 141.
[17] H.M. Cheung, S. Kurup, Environ. Sci. Technol. 28 (1994) 1619.
[18] H. Nagata, T. Takakura, S. Tashiro, M. Kishida, K. Mizuno, I. Tamori, K. Wakabayashi, Appl. Catalysis B: Environ. 5 (1994) 23.
[19] J.H. Kiefer, R. Sathyanarayana, K.P. Lim, J.V. Michael, J. Phys. Chem. 98 (1994) 12278.
[20] H. Nagata, K. Hirai, K. Okitsu, T. Dohmaru, Y. Maeda, Chem. Lett. (1995) 203.

[21] S.S. Kumaran, K.P. Lim, J.V. Michael, A.F. Wagner, J. Phys. Chem. 99 (1995) 8673.
[22] S. Karmakar, H.L. Greene, J. Cat. 151 (1995) 394.
[23] T.N. Bell, L. Kirszenszteijn, B. Czajka, Cat. Lett. 30 (1995) 305.
[24] R.Y. Lin, J. Economy, Appl. Polym Symp. 21 (1973) 143.
[25] S. Kasaoka, Y. Sakata, E. Tanaka, R. Naitoh, Int. Chem. Eng. 29 (1989) 101.
[26] M.P. Cal, S.M. Larson, M.J. Rood, Environ. Prog. 13 (1994) 26.
[27] S.H. Lin, F.M. Hsu, Ind. Eng. Chem. Res. 34 (1995) 2110.
[28] D.M. Ruthven, Principles of Adsorption and Adsorption of Processes, John Wiley and Sons, New York, 1984.
[29] D. Naden, M. Streat, Ion Exchange Technology, Ellis Horwood, London, 1984.
[30] C.H. Jiang, C.C. Can, C.H. Sung, Ion Exchange Separation Engineering, Tienjing University Press, Tienjing, China, 1992.